For submission to Water Research as a Full Paper

High efficiency removal of phosphate from water by zirconium sulfate-surfactant micelle mesostructure immobilized on polymer matrix

Niti Pitakteeratham[a], Akira Hafuka[a], Hisashi Satoh[a,*], and Yoshimasa Watanabe[b]

[a] Division of Environmental Engineering, Faculty of Engineering, Hokkaido University, North-13, West-8, Sapporo 060-8628, Japan

[b] Research Center for Environmental Nano and Bio Engineering, Hokkaido University, North-13, West-8, Sapporo 060-8628, Japan

E-mail:

Niti Pitakteeratham; iamniti_p@hotmail.com

Akira Hafuka; hafuka@eng.hokudai.ac.jp

Hisashi Satoh; qsatoh@eng.hokudai.ac.jp

Yoshimasa Watanabe; yoshiw@eng.hokudai.ac.jp

*Corresponding author.

Hisashi Satoh, Division of Environmental Engineering, Faculty of Engineering, Hokkaido University, North-13, West-8, Sapporo 060-8628, Japan. Tel: +81-(0)11-706-6277 Fax: +81-(0)11-706-6277 E-mail: qsatoh@eng.hokudai.ac.jp

ABSTRACT

A zirconium sulfate-surfactant micelle mesostructure (ZS) was synthesized to investigate its capacity for phosphate removal from water. Its phosphate adsorption kinetics, the effect of pH and interfering anions, adsorption isotherm, desorption capacity, and reusability were investigated. The adsorption isotherms could be described by the Langmuir model. The ZS was an effective adsorbent for phosphate with a very high adsorption capacity (114 mg P/g ZS). The phosphate adsorption capacity increased with decrease in pH. Although the adsorption of nitrate, chloride and acetate ions was negligible, bicarbonate ions were found to be possible interfering anions. The adsorbed phosphate was desorbed effectively using NaOH solution. Since breakage of ZS particles resulted when using NaOH, ZS was immobilized on a polymer matrix and a 50-cycle adsorption-desorption test was carried out to determine the ZS-immobilized polymer (P-ZS) reusability. The P-ZS retained its functionality and adsorption and desorption capacity over 50 cycles without loss of original capacity. A phosphate solution containing about 10 mg P/L was treated in a column packed with P-ZS. The phosphate could be adsorbed completely onto P-ZS up to 1020 bed volumes. These results indicate clearly that ZS is a highly effective adsorbent for phosphate and enables the removal of phosphate from water.

Keywords: Adsorption isotherm; pH effect; Interfering anions; Desorption; Repeated use; Column test

1. Introduction

Since phosphate is an essential nutrient for the growth of organisms in most

ecosystems, it is used in agriculture and other industries (Gilbert, 2009). Its extensive use yields large amounts of phosphate-containing wastewater, which can be released from many point and non-point sources such as agricultural fertilizer runoff, treated and untreated municipal wastewater, and effluents from chemical and food processing industries (Barca et al. 2012). The release of phosphate into water bodies, such as bays, lakes, ponds, lagoons, rivers and seas, is of environmental concern as it can lead to a deterioration in water quality. Phosphate can disturb the ecological balance of an aquatic environment by enhancing algae proliferation, termed eutrophication, and the subsequent depletion of dissolved oxygen, as the algae decay (Camargo et al. 2005). The depletion of dissolved oxygen in water bodies has a harmful effect on fish and other aquatic life, resulting in a reduction in biodiversity (Biswas et al. 2008; Guan et al. 2011).

Owing to the more stringent regulation of phosphate discharge, it is essential to develop effective treatment methods for phosphate removal from phosphate-containing wastewater prior to its discharge into water bodies. Furthermore, phosphorus is known to be a limited resource (Gilbert, 2009; Cordell et al. 2009). Published reports demonstrate that the life time of exploitable reserves of phosphate rock ranges from the next few decades (Yoshida and Galinada, 2002) to several hundreds of years (Bloecher et al. 2012). Hence, phosphorus recovery from phosphate-containing wastewater as an alternative source of phosphate becomes increasingly important to compensate for such global exhaustion of high-grade phosphate ores (Bloecher et al. 2012).

Conventional methods for phosphate removal from water include chemical precipitation (Barat et al. 2011), biological processes (Oehmen et al. 2010), and adsorption processes (Choi et al. 2012, Pan et al. 2009, Genz et al. 2004, Goh et al. 2008).

Among these methods, adsorption techniques are promising, owing to the production of less sludge, simple and easy operation, and high efficiency (Choi et al. 2012). Many adsorbents derived from iron(III), aluminum, zirconium, and manganese(IV) have been reported to be effective in phosphate adsorption (Pan et al. 2009, Genz et al. 2004, Goh et al. 2008). Among these metals, zirconium is a superior adsorbent owing to its strong surface complexing ability for phosphate and high chemical stability under acidic and basic conditions (Chitrakar et al., 2006; Biswas et al., 2008; Liu et al., 2008; Ohura et al., 2011; Yeon et al. 2008). For example, Biswas et al. (2008) reported on the high adsorption capacity of phosphate on orange waste gel loaded with zirconium. Liu et al. (2008) described the effective adsorption of phosphate on mesoporous zirconium oxide. Yeon et al. (2008) synthesized the mesoporous structures of zirconium sulfate by using a template of surfactants which showed higher adsorption capacity for phosphate than those for the adsorbents based on zirconium hydroxides and oxides.

In this study, we synthesized a zirconium sulfate-surfactant micelle mesostructure (ZS) and its phosphate adsorption kinetics, the effect of pH and interfering anions, adsorption isotherm, and desorption capacity were investigated. Furthermore, ZS was immobilized on a polymer matrix and a 50-cycle adsorption-desorption test was carried out to determine the ZS-immobilized polymer (P-ZS) reusability. Finally, a solution containing phosphate was treated using a ZS-packed column.

2. Materials and methods

2.1 Material preparation

We followed the previous work by the same author (Takada et al. 2004) and ZS was

prepared according to the procedure reported in the previous paper. Briefly, 48.5 g of $Zr(SO_4)_2 \cdot 4H_2O$ (Soekawa Chemical Co. Ltd., Tokyo, Japan) and 24.64 g of hexadecyl-trimethylammonium bromide (C_{16}TMABr; Wako Pure Chemical Industries, Ltd., Osaka, Japan) were dissolved in 160 and 838.5 mL of Milli-Q™ water, respectively. The zirconium solution was added dropwise to the C_{16}TMABr solution using a titration technique under continuous stirring over 2 h. The mixture was stirred continuously overnight and then autoclaved at 110°C for 48 h. After crystallization, the white powder product was collected by filtration with Whatman GF/B filter paper, washed repeatedly with Milli-Q water, dried at 80°C for 24 h, and ground into fine powder.

The resulting material, a zirconium sulfate-surfactant micelle mesostructure (abbreviated as ZS), was immobilized on a polymer (Aramid-Polymer). ZS (8 wt%) and the polymer (8 wt%) were added to solvent (N-methyl-2-pyrrolidone) (84 wt%) and mixed at room temperature. The obtained mixture was dropped into coagulation liquid (98 wt% water and 2 wt% N-methyl-2-pyrrolidone). In this manner, the porous polymer-coated ZS particles with ZS/polymer ratio of 8 to 2 (abbreviated as P-ZS) were formed as a result of the spinodal decomposition. The morphology of P-ZS was characterized by a scanning electron microscopy (SEM, Hitachi High-Tech Fielding Co. S-2400).

2.2 Adsorption kinetics

Batch mode adsorption experiments were carried out to examine the adsorption behavior of phosphate on ZS and P-ZS. Briefly, 200 mg each of ZS and P-ZS (corresponding to 160 mg ZS) were introduced into a 500 mL flask with 200 mL varying

concentrations of phosphate standard solutions prepared using Milli-Q water. Three drops of chloroform were added to each flask to inhibit bacterial growth. The initial phosphate standard solution pH was adjusted to 7.0 by adding NaOH or HCl to minimize pH variations owing to the different amounts of KH_2PO_4 added. The solutions were shaken continually at 25°C for 180 min to achieve adsorption equilibrium (i.e., no further uptake) based on determined adsorption kinetics (see Section 3.2). Adsorbent-free controls were run in parallel. During the adsorption process, a 1 mL sample was withdrawn at preset time intervals. After the sample had been filtered using a 0.2 μm pore size membrane (Advantec Co., Ltd., Tokyo, Japan), the phosphate concentration in the solution was determined using a high-performance liquid chromatography system (LC-10AD system; Shimadzu Co., Kyoto, Japan) equipped with Shimadzu Shim-pack SCR-102H column (0.8 × 30 cm) (Bandara et al. 2011; Bandara et al. 2012).

The phosphate equilibrium adsorption amount (i.e., adsorption capacity) was calculated according to:

$$q_e = \frac{(C_0 - C_e)V}{m}, \quad (1)$$

where q_e is the equilibrium adsorption amount (mg P/g ZS), C_0 is the initial phosphate concentration (mg P/L), C_e is the equilibrium phosphate concentration (mg P/L), V is the solution volume (L) and m is the adsorbent mass (g ZS).

The equilibrium adsorption amounts were analyzed using two kinetic models: pseudo-first and -second order kinetics (Velghe et al., 2012; Ho, 2006). Lagergren's rate equation is usually used to describe pseudo-first order kinetics:

$$\log(q_e - q_t) = \log(q_e) - \frac{k_1}{2.303}t, \quad (2)$$

Pseudo-second order kinetics can be expressed as follows:

$$\frac{t}{q_t} = \frac{1}{k_2 q_e^{\,2}} + \frac{1}{q_e} t \,, \qquad (3)$$

where q_t is the amount of phosphate adsorbed per unit weight of adsorbent (mg P/g ZS) at time t, and k_1 and k_2 are the pseudo-first (per minute) and -second order rate constants (g/(mg min)), respectively.

2.3 Effect of pH and possible interfering anions

Separate sets of experiments were conducted in the batch mode adsorption experiments as described above to investigate the effect of solution pH on phosphate adsorption to P-ZS. The fluctuation of solution pH was adjusted within 0.1 of pH unit throughout the test period using 0.1 M HCl or NaOH. The initial phosphate concentration was 160 mg P/L (5 mM).

The adsorption capacity of possible interfering anions on P-ZS was examined. Batch mode adsorption experiments were conducted as described above. P-ZS was introduced into a 500 mL of a flask with 200 mL of Milli-Q water containing 10 mM each of bicarbonate, nitrate, chloride and acetate. The pH was adjusted to 7.0.

2.4 Adsorption isotherms

Adsorption isotherm experiments were carried out during the batch mode adsorption experiments as described above. The phosphate adsorption data were fitted to the Langmuir and Freundlich isotherm models (Zeng et al. 2004) in Eqs (4) and (5), respectively:

$$q_e = \frac{Q_m b C_e}{1 + b C_e} \,, \text{ and} \qquad (4)$$

$$q_e = KC_e^{1/n}, \quad (5)$$

where Q_m is the maximum adsorption capacity (mg P/g ZS), K is a constant related to the adsorption capacity (mg P/g ZS), and b and n are constants related to the energy of adsorption.

2.5 Desorption of phosphate and repetition of adsorption-desorption cycles

Phosphate desorption was studied using a phosphate-loaded ZS, prepared by treatment of 326 mg P/L (10 mM) of a phosphate solution as described above. The phosphate-loaded ZS (1 g) was immersed in 50 mL NaOH solution for 30 min at various solution pH values. During the desorption process, a 1 mL sample was taken at preset time intervals. After the sample had been filtered through a 0.45 μm pore size membrane (Advantec Co., Ltd., Tokyo, Japan), the phosphate concentration in solution was determined as described above. The amount of desorbed phosphate was determined based on the amount of phosphate in solution.

The P-ZS adsorption-desorption cycles were repeated 50 times to determine the P-ZS reusability. In the adsorption test, 326 mg P/L phosphate solution at pH 7.0 was used and the adsorbed phosphate was desorbed at pH 13.5.

2.6 Column-mode adsorption experiments

Continuous phosphate adsorption tests were carried out to investigate the dynamic phosphate breakthrough behavior using a transparent glass column (3.5 cm inner diameter, 53 cm high) fitted with a support at the bottom. Two types of solution were tested: a phosphate standard solution and groundwater. They were pumped separately up-flow

through each column. The columns were equipped with a jacket surrounding the column to maintain the temperature at 25°C. P-ZS (25 g, corresponding to 100 mL) was first soaked in Milli-Q water and then packed into each column. The phosphate standard solution, containing 10 mg P/L of phosphate at pH 7.0, or the groundwater was percolated through the column at 50 mL/h using a peristaltic pump (SJ-1211, ATTO Corporation, Tokyo, Japan). The groundwater phosphate concentration was about 10 mg P/L with a pH of 8.2. The presence of phosphate ions in the groundwater results from the dissolution of phosphate-bearing minerals at the sampling site. The column had been conditioned beforehand using Milli-Q water at the same pH. The effluent was collected at arbitrary time intervals to measure phosphate concentration.

3. Results and discussion

3.1 Characterization of ZS

We followed the previous work by the same author to prepare ZS (Takada et al. 2004). Samples of ZS powder were characterized by XRD, TEM, ICP, and elemental analysis in previous studies (Wu et al., 2005; Iwamoto et al., 2002). The ZS powders showed characteristic (100), (110), and (200) XRD diffractions of the hexagonal structure with d-spacings of 4.28–4.06, 2.47–2.36, and 2.17–2.03 nm. The chemical formula of ZS could be supposed as $Zr(HSO_4)$-$(OH)_{3.5}(C_{19}H_{42}N)_{0.5}\cdot 2H_2O$. A schematic illustration of the ZS structure is depicted in Figure 1. ZS has a regular array of surfactant micelles and contains hydrogen sulfate ions (HSO_4^-) in its wall (Takada et al., 2004). This HSO_4^- can be exchanged with other types of anions such as arsenate, arsenite (Iwamoto et al., 2002) and selenite (Takada et al., 2004) in an aqueous solution. Phosphate resembles arsenate in some

respects because they occupy the same column of the periodic table. Thus we expected that ZS would be a good to excellent anion-exchanger for the phosphate ion.

3.2 Kinetic study

Figure 2 shows the adsorption kinetics of ZS and P-ZS for phosphate. Although the adsorption of both ZS and P-ZS was time dependent, their kinetic profiles for phosphate were different. As expected, the sorption kinetics of ZS for phosphate were rapid and equilibrium was reached within 60 min, while it took 120 min for P-ZS to achieve equilibrium. The slower kinetics of P-ZS compared with ZS probably results from mass transfer resistance within the polymer structure. However, the contact time of 120 min is likely sufficient for P-ZS to achieve adsorption equilibrium. It was noted that the adsorbed amount of phosphate per unit mass of ZS in equilibrium (q_e) was comparable between the ZS and P-ZS.

The kinetic parameters evaluated according to the pseudo-first and -second order equations are listed together with the coefficients of determination in Table 1. As shown in Figure 2 and Table 1, the pseudo-second order model fitted the experimental data better than the pseudo-first order model based on the correlation coefficient (r^2). The good fit ($r^2 > 0.997$) obtained using the second order model indicates that the adsorption of phosphate onto ZS and P-ZS conformed to the chemical reaction mechanisms (Ho and McKay, 1999).

3.3 Effect of pH and possible interfering anions

Figure 3 illustrates the effect of solution pH on phosphate adsorption to P-ZS. As observed, the phosphate adsorption capacity increased with decrease in pH. The maximum phosphate adsorption capacity was 36 mg P/g ZS at pH 3.0. Considering the acid

dissociation constant values of phosphoric acid (pKa_1 = 2.16, pKa_2 = 7.20 and pKa_3 = 12.35) (Benjamin, 2002), the fraction (α_i) of each phosphate species (H_3PO_4, $H_2PO_4^-$, HPO_4^{2-} and PO_4^{3-}) of the total phosphate, which was defined as the sum of H_3PO_4, $H_2PO_4^-$, HPO_4^{2-} and PO_4^{3-}, was calculated (Figure 3). An increase in pH from 7.2 inevitably makes the phosphate species more negatively charged, i.e., it results in the formation of more HPO_4^{2-} (α_2) than $H_2PO_4^-$ (α_1), indicating preferable adsorption of $H_2PO_4^-$ to ZS. This result indicates that phosphate removal by ZS requires pH adjustment to optimize phosphate removal efficiency.

The wastewater and environmental water can contain common anions (for example, bicarbonate, nitrate, chloride and acetate), which may compete with the target phosphate for adsorption sites thereby reducing the adsorption capacity of P-ZS. Therefore, the adsorption kinetics of P-ZS were investigated for bicarbonate, nitrate, chloride and acetate. The uptake (q_e) and distribution coefficients (K_d) of these anions are calculated from the data. K_d can be estimated as follows:

$$K_d \text{ (ml/g)} = q_e \text{ (mmol/g)} / C_e \text{ (mmol/ml)}, \quad (6)$$

where C_e represent the phosphate concentration in solution at equilibrium.

The values of q_e were 0.97 mmol/g-ZS (phosphate), 10^{-3} mmol/g-ZS (chloride), 10^{-2} mmol/g-ZS (nitrate), 0.1 mmol/g-ZS (acetate), and 0.94 mmol/g-ZS (bicarbonate). A higher K_d value was observed for phosphate than for the other anions except for bicarbonate. The selectivity order based on the K_d values was phosphate (K_d = 3390) ≈ bicarbonate (K_d = 3340) >> nitrate (K_d = 109) ≈ acetate (K_d = 84) > chloride (K_d = 1.7). The selectivity of ZS was comparable to that of an adsorbent reported in another study (Chitrakar et al., 2006). These results indicate that P-ZS has a high selectivity toward phosphate, but bicarbonate

should be considered as a possible interfering anion.

3.4 Adsorption isotherms

Adsorption isotherm experiments were performed at pH 7.0 for 180 min, which is sufficient to reach equilibrium according to the kinetic studies as described above (Figure 2). Figure 4 shows phosphate adsorption isotherms onto ZS and P-ZS in two different background solutions, i.e., in the absence or presence of the interfering bicarbonate. The isotherms are characterized by a steep initial rise followed by a plateau, indicating that the shapes of the curves appear Langmuirian in nature (Naeem et al., 2007). The experimental data were analyzed with Langmuir and Freundlich adsorption isotherm models. The Langmuir model assumes the adsorbent surface to be homogenous and the adsorption energies for each adsorption site to be equivalent (Naeem et al., 2007). Solute immobilization occurs without mutual interactions between the molecules adsorbed at the surface. Conversely, the Freundlich model is based on an exponential distribution of adsorption sites and energies, and mutual interaction between adsorbed molecules is possible (Naeem et al., 2007). As shown in Table 2, the values of both the correlation coefficients (r^2) demonstrate that the data are better fitted to the Langmuir equation than the Freundlich equation. The maximum phosphate adsorption capacities of ZS and P-ZS were estimated to be 114 mg P/g ZS for ZS, 110 mg P/g ZS for P-ZS and 67 mg P/g ZS for ZS in the phosphate solution containing bicarbonate, at an equilibrium concentration of about 1450 mg P/L. The lower maximum phosphate adsorption capacity of P-ZS compared with ZS may result from complete immobilization of a part of ZS within the polymer structure. Such a high adsorption capacity has not been reported previously (Table 2). For example,

phosphate adsorption capacity of P-ZS was 30 mg P/g ZS at 9 mg P/L of equilibrium concentration (Figure 4). Hence, P-ZS should be applicable for advanced wastewater treatment of industrial wastewaters (Chimenos et al. 2006; Chimenos et al. 2003) and supernatant of anaerobically digested wastewater sludge (van Rensburg et al. 2003).

3.5 Desorption of adsorbed phosphate from P-ZS and reuse of P-ZS

The applicability of P-ZS as a potential adsorbent depends not only on the adsorption capacity, but also on the desorption performance, which eventually leads to its reusability. Since the mechanism of adsorption of phosphate onto ZS is by ion-exchange, the anion could be considered as a desorption reagent for the adsorbed phosphate. It has been reported that hydroxide is the hardest Lewis base among common inorganic anions (Awual et al., 2011). Therefore, aqueous NaOH behaves as an effective reagent for desorption (Zhu and Jyo, 2005). Figure 5 shows phosphate desorption efficiency at a variety of pH values of the desorption reagent. Phosphate adsorbed on ZS could be desorbed with aqueous NaOH within 10 min (data not shown). The data shown in Figure 5 were taken after 30 min of the desorption process. The phosphate desorption efficiency increased as pH increased to 13.3 and was unchanged above 13.3. The maximal phosphate desorption efficiency was about 85%. These results indicate that ZS can be regenerated. Phosphate desorption may occur through an ion-exchange mechanism involving the release of phosphate and the uptake of hydroxide (Iwamoto et al., 2002). Furthermore, shift of phosphate species from HPO_4^{2-} (α_2) to PO_4^{3-} (α_3) might also affect desorption of phosphate from ZS, because ZS adsorbed preferably HPO_4^{2-} as compared with PO_4^{3-} (Figure 3). Results from the desorption study also indicate that phosphate adsorption on ZS is not completely reversible. In addition, the

bonding between ZS and adsorbed phosphate is probably strong under neutral pH conditions and it is relatively difficult for the adsorbed phosphate to be desorbed.

Although phosphate was desorbed effectively from ZS using NaOH solution, the breakage of ZS particles occurred and the ZS size regenerated with NaOH was below 0.5 μm (data not shown). This change in particle size compromised the reusability of ZS. To recover the smaller size of ZS efficiently, the P-ZS was prepared and its reusability investigated. Adsorbed phosphate on the P-ZS was desorbed by aqueous NaOH solution at pH 13.5. The adsorption-desorption cycles were repeated 50 times and results on phosphate adsorption and desorption capacities are shown in Figure 6. The phosphate adsorption and desorption capacities fluctuated, but there is no trend showing decrease in the adsorption and desorption capacities, indicating that P-ZS could retain functionality and adsorption and desorption capabilities over the 50 cycles without any loss of original efficiency. The total amount of phosphate adsorbed and desorbed over 50 cycles was 1260 and 1100 mg P/g P-ZS, respectively. Although the dry weight of P-ZS decreased to 55 % over the five initial cycles, no measurable loss of P-ZS occurred thereafter. It is probably because washout of the small size of P-ZS (i.e., P-ZS powder) occurred and leakage of ZS from P-ZS was insignificant. The morphology of P-ZS was obtained by SEM. As can be seen, the ZS particles exhibited angular outline and sharp edges (Figure IA in the supplementary data). The images showed that the dimensions of ZS were in the range of 20 to 100 μm. However, still some smaller size ZS existed. ZS was densely packed with polymer. P-ZS had considerable numbers of pores and skin surface (Figure IB in the supplementary data), which could prevent leakage of ZS particles that were broken down during the desorption process. Owing to the high adsorption capacity of ZS to phosphate and its reusability over

many operating cycles without noticeable deterioration, the relatively high cost of the P-ZS raw materials (i.e., zirconium sulfate) will not be a barrier in practical applications.

3.6 Column-mode adsorption experiments

To further evaluate the phosphate removal capacity of P-ZS, column experiments were conducted on a phosphate standard solution (10 mg P/L at pH 7.0). Figure 7 shows breakthrough profiles of phosphate, using columns packed with P-ZS in continuous-mode operation where the solutions were percolated continuously at a hydraulic retention time of 2 h. From this result, it is perceived that breakthrough, which is defined as the point where the phosphate concentration exceeded the analytical detection limit (0.1 mg P/L), occurred at 1020 bed volumes for the phosphate solution. This means that phosphate could be completely adsorbed onto P-ZS (with more than 99 % efficiency) up to the mentioned bed volumes. These values were much higher than those reported in other studies (Biswas et al., 2008; Ohura et al., 2011; Awual et al., 2011). The effective adsorption capacity for P-ZS calculated from the breakthrough profile for the phosphate standard solution was 52 mg P/g ZS, which was almost identical to that (50 mg P/g ZS) evaluated in the batch test (Figure 4).

4. Conclusions

We synthesized a zirconium sulfate-surfactant micelle mesostructure (ZS) as an adsorbent for phosphate removal from water. ZS could adsorb phosphate in water by an ion-exchange process with high adsorption capacity as compared with other phosphate adsorbents. The phosphate adsorption capacity increased with decrease in pH. Bicarbonate was the sole interfering anion among the anions tested. Phosphate adsorbed could be

desorbed from the ZS using NaOH solution. The P-ZS could be regenerated at least 50 times without loss of original functionality. A column packed with P-ZS could remove phosphate completely in a phosphate solution including about 10 mg P/L of phosphate up to 1020 bed volumes, respectively. Therefore, we concluded that ZS was a highly effective adsorbent for phosphate and enabled the removal of phosphate from water.

Acknowledgements

The authors thank Prof. Masakazu Iwamoto for technical support for synthesis of ZS. This research was supported financially by the Core Research of Evolutional Science & Technology (CREST) for "Innovative Technology and System for Sustainable Water Use" from the Japan Science and Technology Agency (JST). The authors would like to specially thank TEIJIN LIMITED for technical support for immobilization of ZS onto polymer.

References

Awual, M.R., Jyo, A., Ihara, T., Seko, N., Tamada, M. and Lim, K.T. (2011) Enhanced trace phosphate removal from water by zirconium(IV) loaded fibrous adsorbent. Water Research 45(15), 4592–4600.

Bandara, W.M.K.R.T.W., Satoh, H., Sasakawa, M., Nakahara, Y., Takahashi, M., Okabe, S. (2011) Removal of residual dissolved methane gas in an upflow anaerobic sludge blanket reactor treating low-strength wastewater at low temperature with degassing membrane. Water Research 45(11), 3533–3540.

Bandara, W.M.K.R.T.W., Kindaichi, T., Satoh, H., Sasakawa, M., Nakahara, Y.,

Takahashi, M., Okabe, S. (2012) Anaerobic treatment of municipal wastewater at ambient temperature: Analysis of archaeal community structure and recovery of dissolved methane. Water Research in press.

Barat, R., Montoya, T., Seco, A., Ferrer, J. (2011) Modelling biological and chemically induced precipitation of calcium phosphate in enhanced biological phosphorus removal systems. Water Research 45(12), 3744–3752.

Barca, C., Gerente, C., Meyer, D., Cliazarenc, F. and Andres, Y. (2012) Phosphate removal from synthetic and real wastewater using steel slags produced in Europe. Water Research 46(7), 2376–2384.

Benjamin, M.M., 2002. Water Chemistry. McGraw-Hill, New York, NY.

Biswas, B.K., Inoue, K., Ghimire, K.N., Harada, H., Ohto, K. and Kawakita, H. (2008) Removal and recovery of phosphorus from water by means of adsorption onto orange waste gel loaded with zirconium. Bioresource Technology 99(18) 8685–8690.

Bloecher, C., Niewersch, C. and Melin, T. (2012) Phosphorus recovery from sewage sludge with a hybrid process of low pressure wet oxidation and nanofiltration. Water Research 46(6), 2009–2019.

Camargo, J.A., Alonso, K. and de la Puente, M. (2005) Eutrophication downstream from small reservoirs in mountain rivers of Central Spain. Water Research 39(14), 3376–3384.

Chimenos, J.M., Fernández, A.I., Villalba, G., Segarra, M., Urruticoechea, A., Artaza, B. and Espiell, F. (2003) Removal of ammonium and phosphates from wastewater resulting from the process of cochineal extraction using MgO-containing by-product. Water Research 37(7), Pages 1601–1607.

Chimenos, J.M., Fernández, A.I., Hernández, A., Haurie, L., Espiell, F. and Ayora, C. (2006) Optimization of phosphate removal in anodizing aluminium wastewater. Water Research 40(1), Pages 137–143.

Chitrakar, R., Tezuka, S., Sonoda, A., Sakane, K., Ooi, K. and Hirotsu, T. (2006) Selective adsorption of phosphate from seawater and wastewater by amorphous zirconium hydroxide. Journal of Colloid and Interface Science 297(2) 426–433.

Choi, J.-W., Lee, S.-Y., Lee, S.-H., Lee, K.-B., Kim, D.-J. and Hong, S.-W. (2012) Adsorption of Phosphate by Amino-Functionalized and Co-condensed SBA-15. Water Air and Soil Pollution 223(5) 2551–2562.

Cordell, D., Drangert, J.-O., White, S. (2009) The story of phosphorus: Global food security and food for thought. Global Environmental Change-Human and Policy Dimensions. 19(2) 292–305.

Genz, A., Kornmuller, A. and Jekel, M. (2004) Advanced phosphorus removal from membrane filtrates by adsorption on activated aluminium oxide and granulated ferric hydroxide. Water Research 38(16) 3523–3530.

Gilbert, N. (2009) Environment: The disappearing nutrient. Nature 461 716–718.

Goh, K.-H., Lim, T.-T. and Dong, Z. (2008) Application of layered double hydroxides for removal of oxyanions: A review. Water Research 42(6–7), 1343–1368.

Guan, B.H., An, S. Q. Gu, B. H. (2011) Assessment of ecosystem health during the past 40 years for Lake Taihu in the Yangtze River Delta, China. Limnology 12(1) 47–53.

Ho, Y.S. (2006) Second-order kinetic model for the sorption of cadmium onto tree fern: A comparison of linear and non-linear methods. Water Research 40(1) 119–125.

Ho, Y.S. and McKay, G. (1999) Pseudo-second order model for sorption processes.

Process Biochemistry 34(5) 451–465.

Iwamoto, M., Kitagawa, H. and Watanabe, Y. (2002) Highly effective removal of arsenate and arsenite ion through anion exchange on zirconium sulfate-surfactant micelle mesostructure. Chemistry Letters 31(8) 814–815.

Liu, H., Sun, X., Yin, C., Hu, C. (2008) Removal of phosphate by mesoporous ZrO_2. Journal of Hazardous Materials 151(2-3) 616–622.

Naeem, A., Westerhoff, P. and Mustafa, S. (2007) Vanadium removal by metal (hydr)oxide adsorbents. Water Research 41(7), 1596–1602.

Oehmen, A., Carvalho, G., Lopez-Vazquez, C.M., van Loosdrecht, M.C.M. and Reis, M.A.M. (2010) Incorporating microbial ecology into the metabolic modelling of polyphosphate accumulating organisms and glycogen accumulating organisms. Water Research 44(17) 4992–5004.

Ohura, S., Harada, H., Biswas, B.K., Kondo, M., Ishikawa, S., Kawakita, H., Ohto, K., Inoue, K. (2011) Phosphorus recovery from secondary effluent and side-stream liquid in a sewage treatment plant using zirconium-loaded saponified orange waste. Journal of Material Cycles and Waste Management 13(4) 293–297.

Pan, B., Wu, J., Pan, B., Lv, L., Zhang, W., Xiao, L., Wang, X., Tao, X. and Zheng, S. (2009) Development of polymer-based nanosized hydrated ferric oxides (HFOs) for enhanced phosphate removal from waste effluents. Water Research 43(17) 4421–4429.

Takada, H., Watanabe, Y. and Iwamoto, M. (2004) Zirconium sulfate-surfactant micelle mesostructure as an effective remover of selenite ion. Chemistry Letters 33(1), 62–63.

Tang, Y., Zong, E., Wan, H., Xu, Z., Zheng, S., Zhu, D. (2012) Zirconia functionalized SBA-15 as effective adsorbent for phosphate removal. Microporous and Mesoporous

Materials 155. 192–200.

van Rensburg, P., Musvoto, E.V,, Wentzel, M.C. and Ekama, G.A. (2003) Modelling multiple mineral precipitation in anaerobic digester liquor. Water Research 37(13) 3087–3097.

Velghe, I., Carleer, R., Yperman, J., Schreurs, S. and D'Haen, J. (2012) Characterisation of adsorbents prepared by pyrolysis of sludge and sludge/disposal filter cake mix. Water Research 46(8) 2783–2794.

Wu, P., Liu, Y.M., He, M.Y. and Iwamoto, M. (2005) Postsynthesis of hexagonally packed porous zirconium phosphate through a novel anion exchange between zirconium oxide mesophase and phosphoric acid. Chemistry of Materials 17(15) 3921–3928.

Yeon, K.H., Park, H., Lee, S.H., Park, Y.M., Lee, S.H. and Iwamoto, M. (2008) Zirconium mesostructures immobilized in calcium alginate for phosphate removal. Korean Journal of Chemical Engineering 25(5) 1040–1046.

Yoshida, H. and Galinada, W. A. (2002) Equilibria for adsorption of phosphates on OH-type strongly basic ion exchanger. AIChE Journal 48(10) 2193–2202.

Zeng, L., Li, X.M. and Liu, J.D. (2004) Adsorptive removal of phosphate from aqueous solutions using iron oxide tailings. Water Research 38(5), 1318–1326.

Zhu, X.P. and Jyo, A. (2005) Column-mode phosphate removal by a novel highly selective adsorbent. Water Research 39(11), 2301–2308.

Figure captions

Figure 1. Schematic illustration of ZS structure.

Figure 2. Adsorption kinetics of ZS and P-ZS for phosphate. ZS, P-ZS and phosphate concentrations were 1 g ZS/L, 0.8 g ZS/L and 50 mg P/L, respectively. Symbols represent the observed kinetics experimental data. Dotted and solid lines are predictions calculated using pseudo-first and -second order equations, respectively.

Figure 3. Effect of pH in the solution at equilibrium on phosphate adsorption to P-ZS. The initial phosphate concentration was 160 mg P/L (5 mM).

Figure 4. Phosphate adsorption isotherms onto ZS and P-ZS. Adsorption isotherm experiments for ZS were performed in the absence and presence of the interfering bicarbonate ion. The initial phosphate concentrations ranged from 3 mg P/L to 1630 mg P/L. Solid lines are predictions calculated using the Langmuir adsorption isotherm model.

Figure 5. Phosphate desorption efficiency at various desorption reagent pH values. The initial phosphate concentration for adsorption test was 326 mg P/L (10 mM). The phosphate-loaded ZS was immersed in 50 mL NaOH solution for 30 min at various solution pH values.

Figure 6. Cumulative adsorption and desorption of phosphate for P-ZS over 50

consecutive adsorption-desorption cycles. The phosphate concentration for adsorption test was 326 mg P/L (10 mM) and pH for desorption test was 13.5.

Figure 7. Breakthrough profiles of phosphate onto P-ZS. C and C_0 are the effluent phosphate concentration at time t and initial concentration, respectively.

Figure I in the supplementary data. SEM images of the cross-section of P-ZS at ×400 (A) and ×60 magnifications (B).

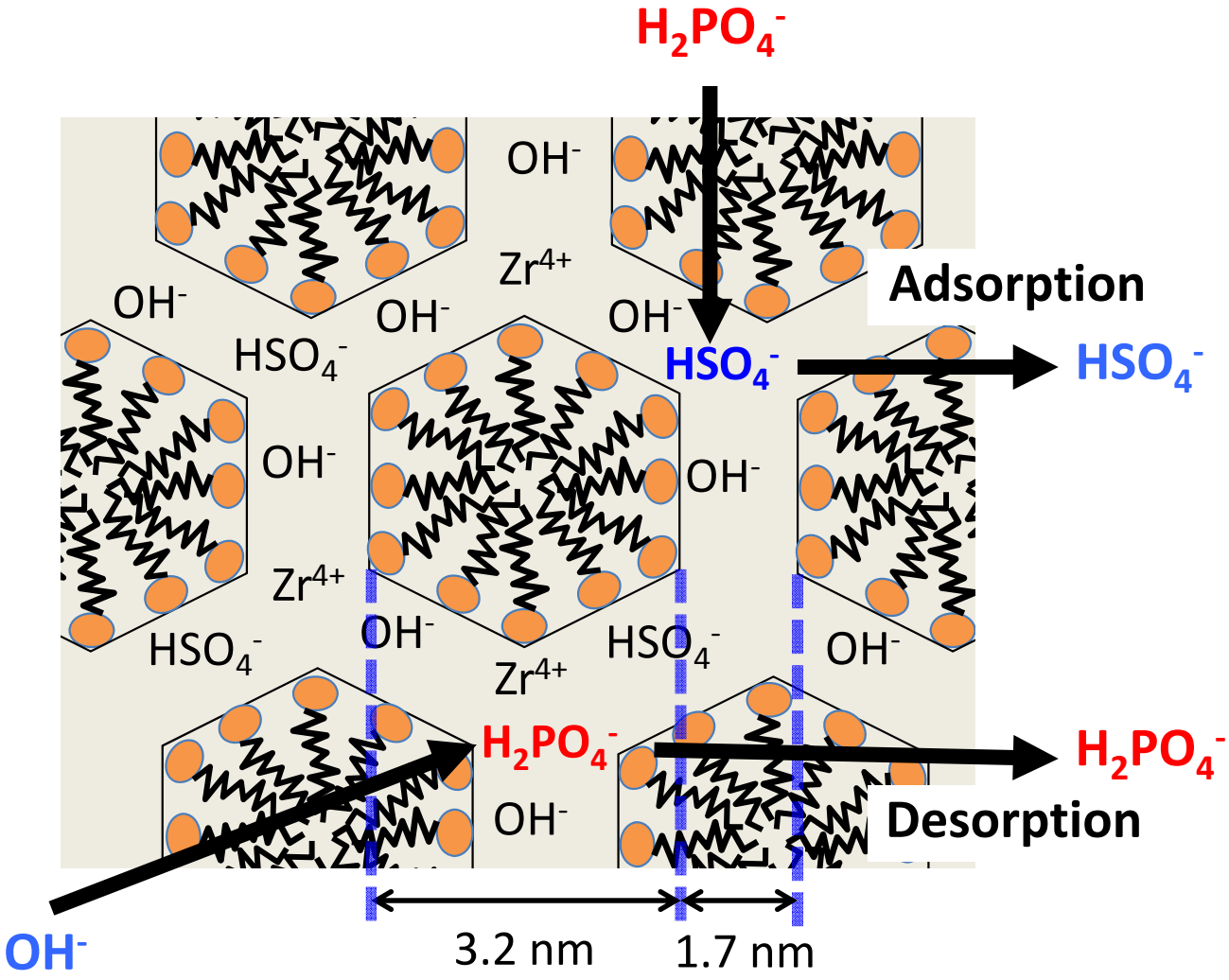

Figure 1
Pitakteeratham et al.

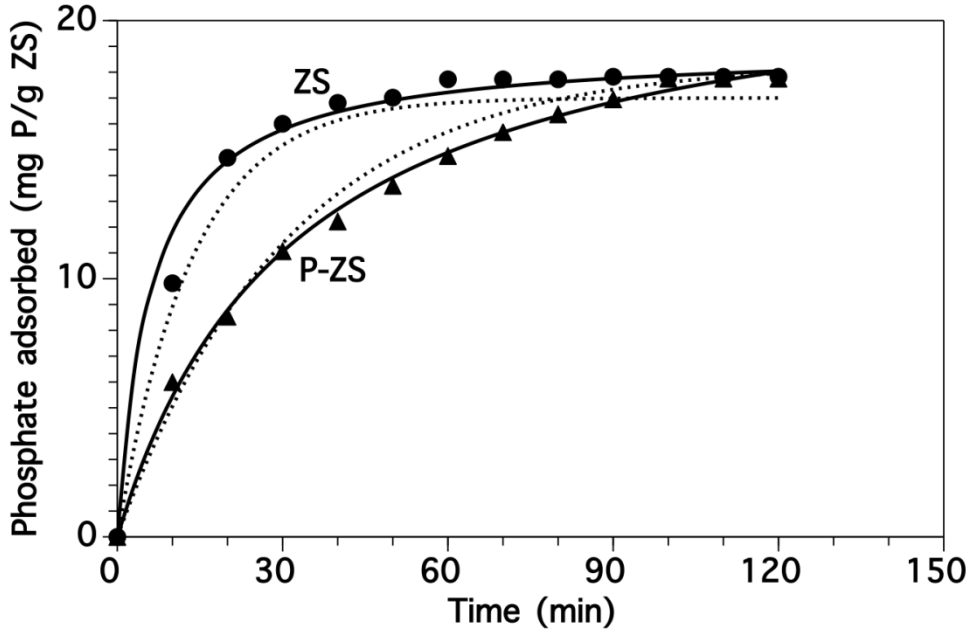

Figure 2
Pitakteeratham et al.

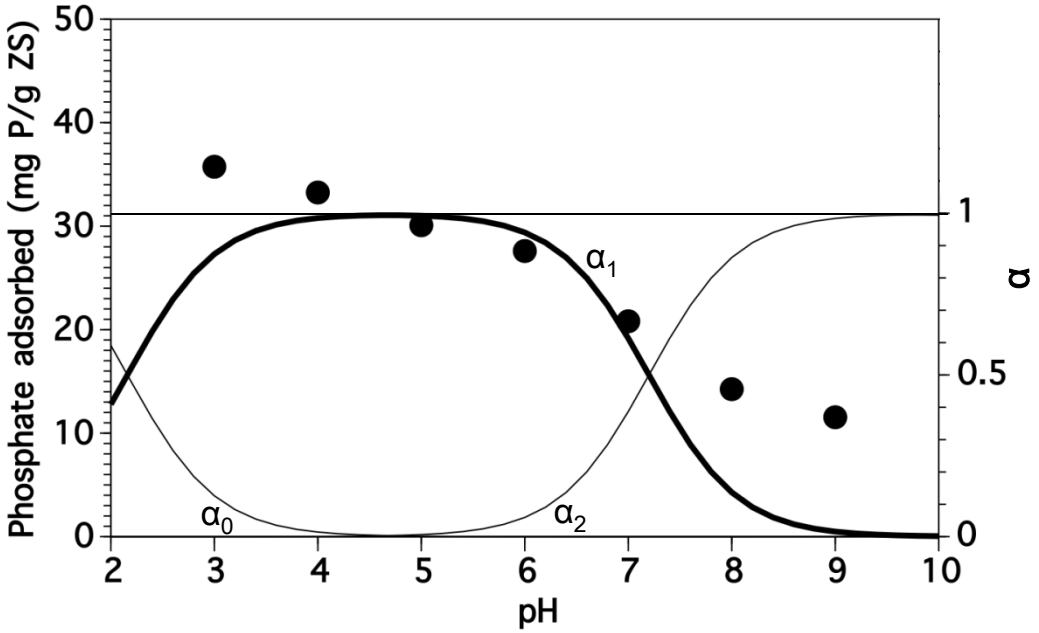

Figure 3
Pitakteeratham et al.

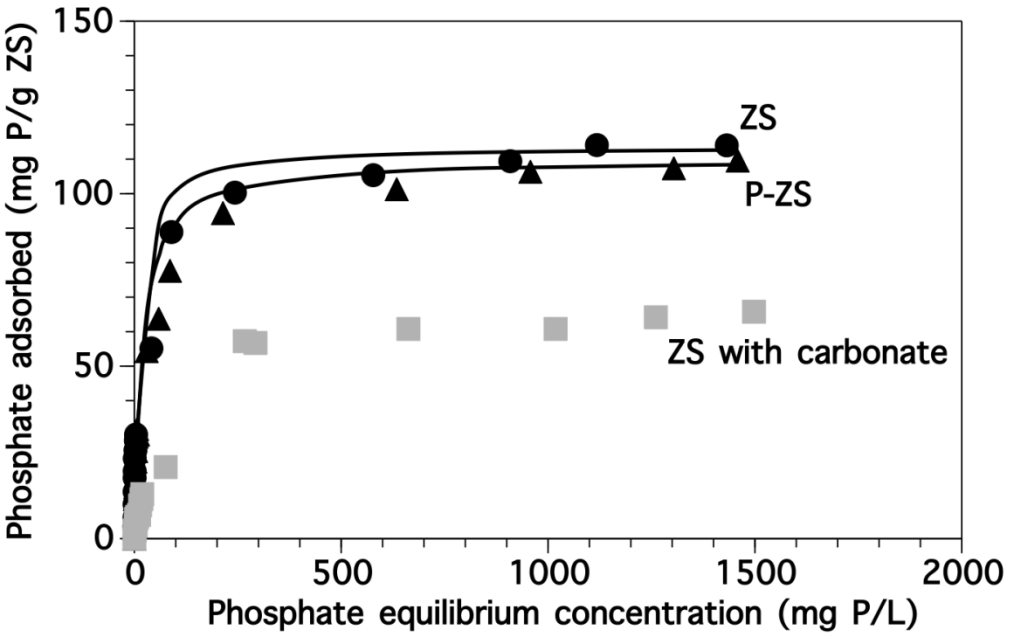

Figure 4
Pitakteeratham et al.

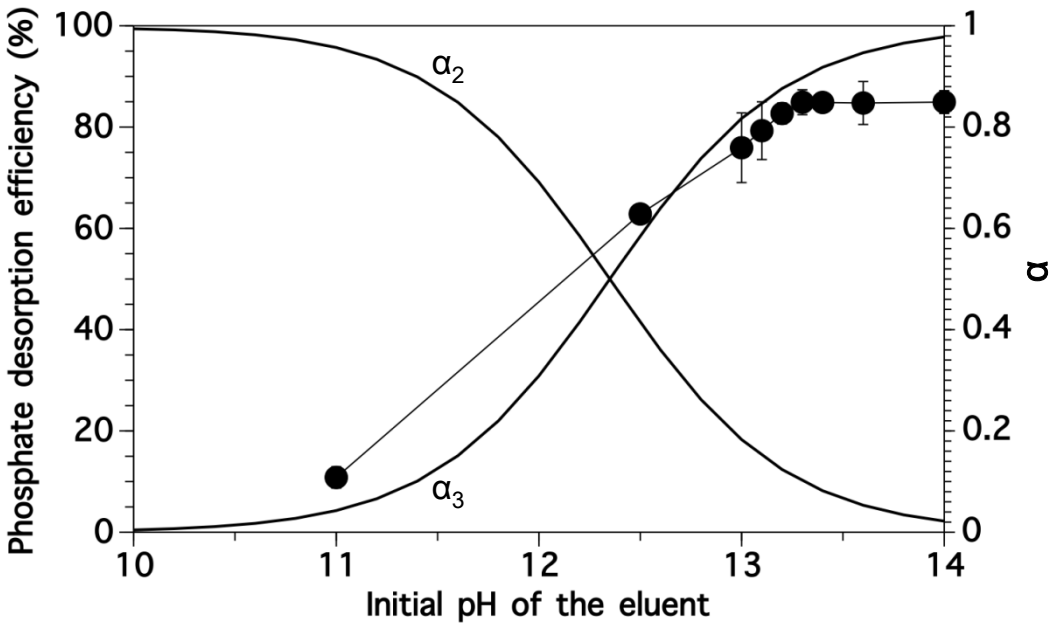

Figure 5
Pitakteeratham et al.

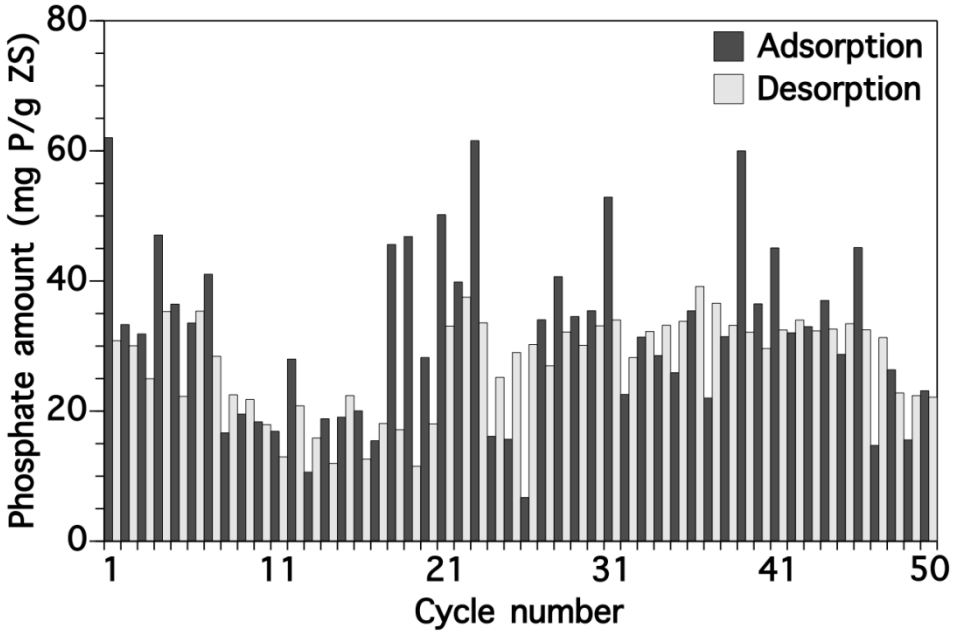

Figure 6
Pitakteeratham et al.

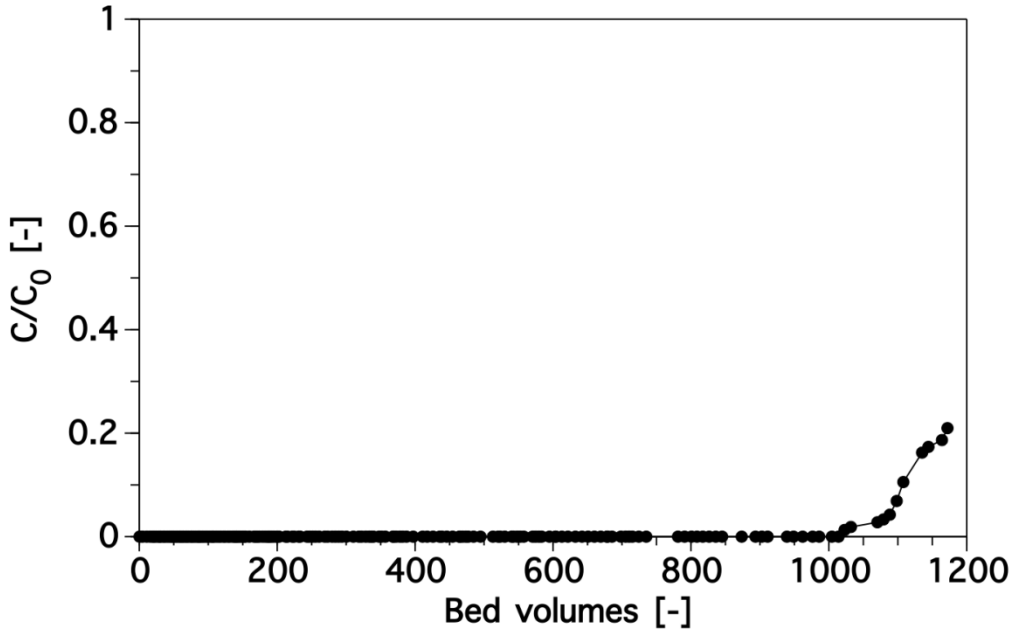

Figure 7
Pitakteeratham et al.

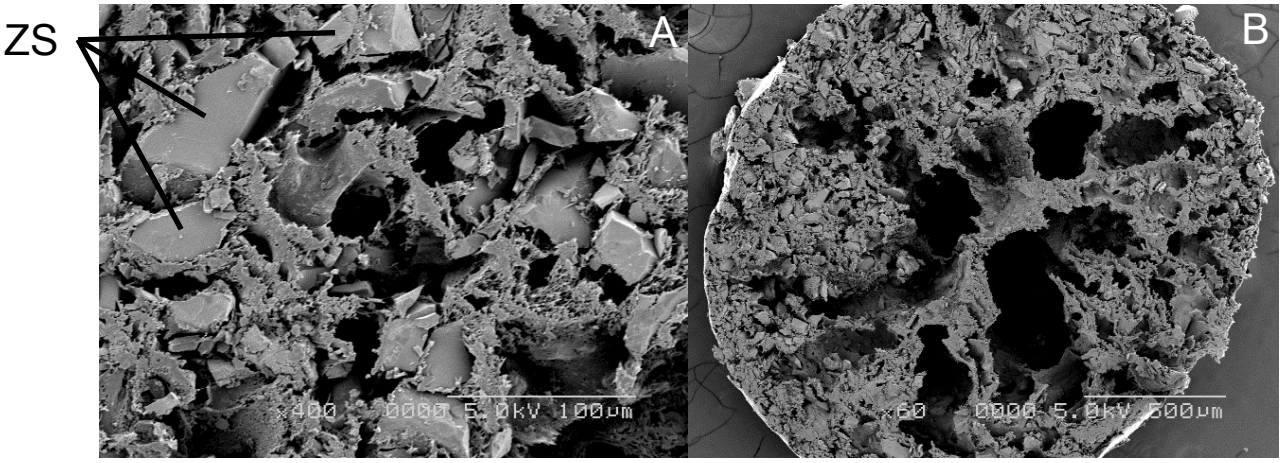

Figure I in the supplementary data
Pitakteeratham et al.

TABLE 1. The kinetic parameters evaluated according to the pseudo-first order and pseudo-second-order equations

Adsorbents	q_{exp} (mg P/g adsorbent)	Pseudo first-order kinetic model			Pseudo second-order kinetic model				Ref.
		q_e (mg P/g adsorbent)	k_1 (min^{-1})	r^2	q_e (mg P/g ZS)	k_2 (g/(mg min))	h (mg P/(g ZS min))	r^2	
ZS	17.8	17.0	0.074	0.941	18.9	0.00874	3.14	0.999	This study
P-ZS	17.8	18.3	0.032	0.982	22.8	0.00137	0.71	0.997	This study
ZrO_2-SBA-15	13.8	8.1	0.002	0.93	14.7	0.0006		0.99	Tang et al., 2012
Zr(IV)-SOW	24.9	18.8		0.96	25.9			0.99	Biswas et al.,
Co-cond.SBA-15	40.0	39.0	0.246	0.983	41.0	0.0141		0.990	~~2012~~2008 ~~Choi et al., 2012~~

h is the initial sorption rate calculated as $k_2 q_e^2$

TABLE 2. Lists of the values of both the Freundlich and Langmuir parameters obtained from the two isotherms with their corresponding correlation coefficients (r^2).

Adsorbents	Langmuir parameters			Freundlich parameters			Ref.
	B (L/mg)	Q_m (mg P/g adsorbent)	r^2	1/n	logK	r^2	
ZS	0.079	114	0.955	0.330	1.17	0.870	This study
P-ZS	0.049	110	0.950	0.393	1.05	0.930	This study
Zr-SOW	0.023	57	0.986				Biswas et al.,
Zr-MUROMAC	0.021	43	0.988				~~2012~~2008
Zirconium ferrite	0.040	13	0.993				Biswas et al.,
Amorphous Zr		17		0.333	1.24	0.998	~~2012~~2008
Mesoporous ZrO_2	0.062	30	0.965				Biswas et al.,
							~~2012~~2008
							Chitrakar et al., 2006